DE GRUYTER OPEN

Mathematical Modelling in Civil Engineering
Vol. 10-No. 1-2014
Doi: 10.2478/mmce-2014-0001

PRELIMINARY WRF-ARW MODEL ANALYSIS OF GLOBAL SOLAR IRRADIATION FORECASTING

DRAGOS ISVORANU- Associate Professor, PhD, University Politehnica of Bucharest, Faculty of Aerospace Engineering, Bucharest, e-mail: ddisvoranu@gmail.com

VIOREL BADESCU- Professor, PhD, University Politehnica of Bucharest, Candida Oancea Institute, Bucharest, e-mail: badescu@theta.termo.pub.ro

Abstract: The purpose of this research is focused on the evaluation of short term global solar irradiation forecasting performance in order to assess the outcome of photovoltaic power stations. The paper presents a comparative analysis between the predicted irradiation obtained by numerical simulation and measurements. The simulation data is obtained from WRF-ARW model (Weather Research Forecasting-Advanced Research WRF), whose initial and boundary conditions are provided by the global forecasting model GFS. Taking into account the complexity of options for the physics models provided with WRF, we embarked upon a parametric analysis of the simulated solar irradiance. This complex task provides a better insight among the coupling of various physics options and enables us to find the best fit with the measured data for a specified site and time period. The present preliminary analysis shows that the accuracy of the computed global solar irradiance can be improved by choosing the appropriate built-in physics models. A combination of physics models providing the best results has been identified.

Keywords: global irradiance forecast, NWP simulation, PV stations, model analysis

1. Introduction

Solar energy has a specific common characteristic: a high variability in space and time. It is highly dependent on the cloud structure, day/night cycles, the humidity and the aerosol load of the atmosphere. Due to intermittent weather patterns, solar energy power plants cannot guarantee the amount of energy which is requested by the electrical grid operators in order to respond at any time to the end users demands. Therefore, secondary energy sources have to be considered locally or on a regional scale. Additionally, weather has a major impact on the electricity transmission and distribution grids, from the risk of outages and transmission capacity on one side and to the end users highly variable and weather dependant demands on the other side.

An increased production of solar energy will lead to a higher number of dispersed production sites with a highly variable weather dependant energy production which is fed into the medium and lower voltage grids. In such systems, production forecasts for the next minutes up to several days ahead are of high importance as they enable the utilities and the grid operators to adapt the load schedule, hence to contribute to an optimized production and distribution of solar energy and make the PV stations more competitive against classical production sources. In this sense, accurate forecasts of solar energy production as well as an optimized implementation of these forecasts for load schedules are of utmost importance.

The objective of the present paper is the assessment of the quality and performance of global solar irradiance forecasting. The paper presents a comparative analysis between the surface global irradiance measured for Romania and the predicted irradiance obtained by numerical simulation. The measured data comes from the Romanian National Meteorological Administration.

2. Solar radiation forecasting

The basic idea of numerical weather prediction is to sample the state of the atmosphere at a given time and use the equations of fluid dynamics and thermodynamics to estimate the state of the fluid at some time in the future. Models are initialized using these observed data. The irregularly spaced observations are processed by data assimilation and objective analysis methods, which perform quality control and obtain values at locations usable by mathematical algorithms of the model (usually on an evenly spaced grid)..

Our primarily research interest lies within the first three meteorological forecasting ranges: now-casting, that is a 0-3 hours description of forecasted weather parameters; very short-range weather prediction (up to 12 hours prediction); Short-range weather forecasting (beyond 12 hours and up to 72 hours description of weather parameters); Medium-range weather forecasting (beyond 72 hours and up to 240 hours description of weather parameters).

Different approaches to forecast irradiance can be taken depending on the target forecasting time. For very short time forecasts (up to 3 h, now-casting), approaches based on extrapolating the solar radiation field from cloud motion have been proposed [1]. In addition, statistical techniques have been proposed for forecasting solar irradiance with up to 24 h [2]. However, Numerical Weather Prediction (NWP) models are the basis of solar yield forecasts with up 48 h time horizon [3], the time range useful for grid integration and decision making in the energy market.

The earliest evaluation studies on the MM5 mesoscale model [4] reliability for estimating global horizontal irradiance (GHI; units:W/m^2) were carried out by Zamora et al. in some locations in USA ([5], [6]). Heinemann et al. [1] evaluated the MM5 model GHI forecasts in Germany for lead time up to 48 h. Lorenz et al. [7] evaluated several NWP-based hourly GHI forecasts in Europe. The same author evaluated GHI forecasts, based on the European Centre for Medium-Range Weather Forecast (ECMWF) NWP model, for power prediction of PV systems in Germany [8]. They reported relative root mean square error (RMSE) values of about 35% for single stations for a 24 h horizon forecasts. Remund et al. [9] evaluated different NWP-based GHI forecasts in the USA, reporting relative RMSE values ranging from 20% to 40% for a 24 h forecast horizon. Similar results were reported by Perez et al. [10], evaluating NWP-based irradiance forecasts in several places in the USA. The Weather Research and Forecasting (WRF) model has a wide range of physical parameterizations, which allow setting the model to better describe the physical processes based on model domain, resolution, location and application [11].

3. WRF presentation

The weather forecast model used in this work for solar radiation forecasting is strongly dependent on the characteristic space scale. The meteorology scale encompasses domains ranging from the synoptic, planetary scale, regional or mesoscale domains covering from 5km to a few hundred kilometers and below 1 km, the meteorology microscale. The most popular synoptic models are GFS, ECMWF, GME, UKMO while HRM, Hirlam, Lokal Model, WRF-NMM, WRF-ARW, Unified Model, MM5 are mesoscale models [12]. Usually, the global models provide the initial and boundary conditions needed to start the regional models but they can also be used directly in the local analysis.

The WRF model [13] is focused on the deterministic estimation of the state of the atmosphere at a future moment in time given the initial state of the system. In order to proceed with this analysis (specifically the radiometric parameters), initial and boundary conditions (mainly lateral conditions) are needed to be generated in the module REAL (Fig. 1) from the raw data provided by the preprocessing module WPS, whose main task is the horizontal interpolation of geographical and meteorological fields extracted from available previous forecast (usually a global forecast). The REAL module performs additional tasks like: defining a vertical coordinate, vertical interpolation, computing a base state/reference profile for the geopotential and column pressure as well as the perturbations from the base state of the previous quantities, etc.

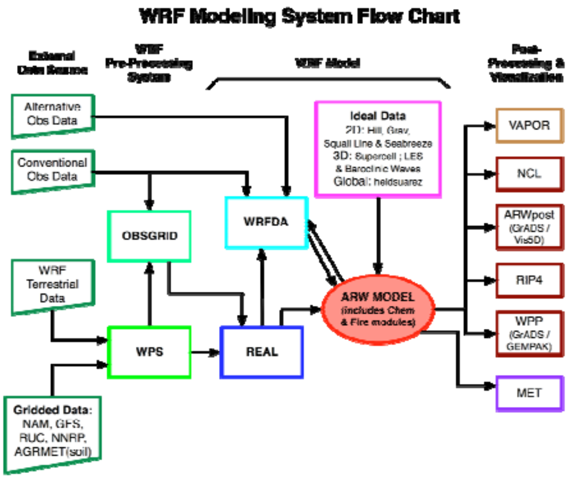

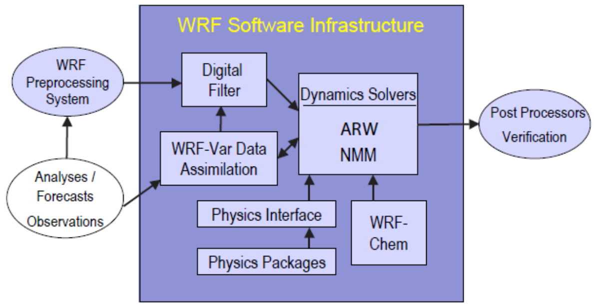

Fig. 1 - Block diagram of the WRF system [13]. **Fig. 2** - Insight in the infrastructure of WRF model [14].

The infrastructure of the WRF system is depicted in Fig. 2. The WRF model comprises two dynamic nuclei, ARW and NMM, the first stemming from the National Center for Atmospheric Research (NCAR) Advanced Research WRF (ARW) and the other one from the National Center for Environmental Predictions (NCEP). The NMM acronym comes from "non-hydrostatic mesoscale model" while ARW from "advanced research weather forecast system". The WRF model is a fully compressible, multi-grid, multi-level, non-hydrostatic Eulerian model with a wide range of microphysics options. Its vertical coordinate is a terrain-following hydrostatic pressure coordinate. The grid staggering is the Arakawa C-grid. The model uses the Runge-Kutta 2^{nd} and 3^{rd} order time integration schemes and 2^{nd} to 6^{th} order advection schemes in both horizontal and vertical coordinate. The dynamics conserves scalar variables. The WRF model version 3 supports a large variety of physics options, various lateral conditions, data assimilation one-way, two-way nesting and moving nests. The main physics interface includes [14]:

- *Microphysics*: Schemes ranging from simplified physics suitable for idealized studies to sophisticated mixed-phase physics suitable for process studies and NWP. Currently there are 13 models: Kessler, Purdue Lin, WSM3, WSM5, WSM6, Eta GCP, Thompson, Goddard, Milbrandt 2-Moment, Morrison 2-Moment, SBU-Ylin, WDM5, WDM6.

- *Cumulus parameterizations*: Adjustment and mass-flux schemes for mesoscale modelling. Nine cumulus schemes are implemented in WRF v.3: Kain-Fritsch, Betts-Miller-Janjic, Grell-Devenyi, Simplified Arakawa-Schubert, Grell-3, Tiedtke, Zhang-McFarlane, New SAS, Old Kain-Fritsch.

- *Surface physics*: Multi-layer land surface models ranging from a simple thermal model to full vegetation and soil moisture models, including snow cover and sea ice. The current models are: 5-layer thermal diffusion, Noah LSM, RUC LSM, Pleim-Xiu LSM.

- *Planetary boundary layer physics*: Provides boundary layer fluxes including turbulent energy budget and vertical diffusion in whole column. The following 11 models are in use: YSU, MYJ, GFS, QNSE, MYNN2, MYNN3, ACM2, BouLac, UW, TEMF, MRF.

- *Atmospheric radiation physics*: Longwave and shortwave schemes with multiple spectral bands and a simple shortwave scheme suitable for climate and weather applications. Cloud effects and surface fluxes are included. There are 6 longwave schemes: RRTM, CAM, RRTMG, New Goddard, Held-Suarez, GFDL and 6 shortwave models: Dudhia [15], Goddard [16], CAM [17], RRTMG [18], New Goddard [19] and GFDL [20].

- *Turbulence/diffusion*: Sub-grid eddy effects on all fields including computation of advection coefficients. There are four options for computing K and two options for horizontal diffusion.

An illustrative block diagram of the interactions among various physics modules is represented in Fig. 3.

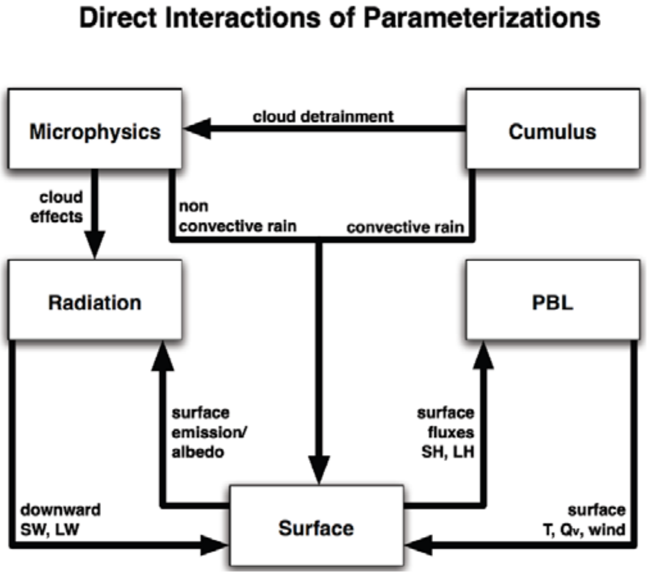

Fig. 3 - Coupling among physics modules [21] .

The popularity of the WRF model has significantly increased even in Europe in the last years. Recently, studies from Spanish meteorological agency have shown that WRF model can be fully integrated as a member of the ensemble forecasting systems [12]. One month simulations of the various physics options of WRF-NMM model using global data from GFS and ECMWF models have shown a relative superiority compared to the results obtained from the Unified Model from UK Meteorological Office and GME from Deutsche Wetterdienst [12].

4. Radiation model

The radiation schemes provide atmospheric heating due to radiative flux divergence and surface downward longwave and shortwave radiation for the ground heat budget. All the radiation schemes in WRF are currently column (one-dimensional) schemes, so each column is treated independently, and the fluxes correspond to those in infinite horizontally uniform planes, which is a good approximation if the vertical thickness of the model layers is much less than the horizontal grid length. The radiation model is closely related with several microphysics options.

Clear-air scattering, water vapour absorption and cloud albedo as well as absorption are usually determined from look-up tables for clouds from Stephens [22]. The downward component of shortwave flux is evaluated taking into account: 1) the effects of solar zenith angle, which influences the downward component and the path length; 2) clouds, which have their own albedo and absorption; 3) and clear air, where there is scattering and water-vapour absorption. Thus, the downward shortwave flux, (units: W/m^2)

$$S_d(z) = \mu S_0 - \int_z^{top} \left(dS_{cs} + dS_{ca} + dS_a + dS_s \right) \quad (1)$$

where μ is the cosine of the zenith angle, S0 is the solar constant (units: W/m^2), z is the current level (units: meters above sea level (m asl)) and top the last level of the model. Subscripts "cs" and "ca" refer to cloud absorption and cloud scattering while "a" and "s" to absorption transmissivity and scattering transmissivity. Cloud fraction in a grid box varies between 0 and 1. WRF schemes use maximum-random overlap policy for multiple layers with varying cloud fraction. The cloud fraction is maximum (1) for neighbouring cloudy layers and random for layers separated by clear sky. The cloud back-scattering (or albedo) and absorption are bilinearly interpolated from tabulated functions of μ and $\ln(w/\mu)$ (where w is the vertically integrated cloud water path) derived from Stephens's theoretical results [18]. The total effect of a cloud or multiple layers of cloud above a height z is found from the above function as a percentage of the downward solar flux absorbed or reflected. Then at a height $z-\Delta z$, a new total percentage is calculated from the table, allowing the effect of the layer Δz to be estimated. However, this percentage is only applied to $\mu S_0 - \Delta S$ (clear air); that is, the clear-air effect above z is removed. Clear-air water vapour absorption is calculated as a function of water vapour path allowing for solar zenith angle. The absorption function is taken from Lacis and Hansen [20]. The method is a similar integration-difference scheme to that described above for cloud. Clear-air scattering is taken to be uniform and proportional to the atmosphere mass path length, again allowing for the zenith angle, with a constant giving 20 percent scattering in one atmosphere [4].

5. Results and discussion

The radiometric measurement data sets were obtained from the following Romanian meteorological stations (see Table 1) supplied with Kipp & Zonen CM6B radiometers [23].

Table 1

Coordination of the Romanian meteorological stations used here

Station name	Latitude (deg N)	Longitude (deg E)	Altitude (m asl)
Timisoara	45.77	21.26	86
Cluj	46.78	23.57	417
Iasi	47.17	27.63	103
Galati	45.47	28.03	71
Craiova	44.31	23.87	192

The measurement uncertainty is ± 5%. The temperature dependence of sensitivity is ±2% on the interval -20 to +40 ºC. On a monthly basis the bias for CM6B ranges between – 2% and +0.9%. The radiometers are checked twice per week and cleaned when necessary. Measurements are performed as follows. Solar irradiance (units: W/m^2) is measured at 1-minute intervals. The series of irradiance values are averaged over 10 minutes, 60 minutes and 1440 minutes, respectively. Irradiation values (units: J) for 10 minutes, one hour and 24 hours are obtained by multiplying the appropriate average irradiance values by the appropriate time duration. Considering the possibilities of interconnecting various physics options one can immediately come across over 30000 different combinations (not counting various sub-options) of switches that might be used as input into WRF code. Of course, a complete parametric analysis should take into account all these options, but it would mean a daunting task that no one could expect to fulfill in a reasonable time horizon. For preliminary testing purposes and based on a prior educated guess, we have reduced the huge number to only 30 different cases to undertake for our analysis. From the numerical point of view we have chosen to use the 3rd order Runge-Kutta procedure for time integration, to use positive horizontal advection option for scalar variables, as well as moisture and turbulent kinetic energy. We employed the full diffusion schemes that use full metric terms for gradients in sloped coordinates and the 6th order horizontal hyper diffusion on all variables to act as a selective short-wave numerical filter. The vertical diffusion was selected to act on full fields not only on the perturbation resulted from the 1D base profile.

Lateral boundary conditions were considered as specified (imposed by REAL module). Due to a relatively coarse grid we used (10 km x 10 km), we chose to employ a PBL scheme in connection with a 2D Smagorinsky model that computes the horizontal diffusion coefficient from the horizontal deformation while the vertical diffusion coefficient results from PBL. The rest of the choices are presented in Table 2.

Table 2

WRF physics options

	Model 1	Model 2	Model 3	Model 4	Model 5
Microphysics (MP)	Morrison 2-Mom.	Thomson	Purdue Lin	-	-
Cumulus parametrization (CP)	New SAS	Grell-3	-	-	-
Surface physics (SP)	Noah LSM+QNSE	-	-	-	-
Planetary Boundary Layer (PBL)	QNSE	-	-	-	-
Longwave Radiation (LR)	CAM	-	-	-	-
Shortwave Radiation (SR)	Goddard	GFDL	CAM	New Goddard	RRTMG

The 30 cases are denoted as follows: from 1 to 5, Model 1 (MP, CP, SP, PBL, LR) and Model 1 to Model 5 from SR; from 6 to 10, Model 1 MP, Model 2 CP, Model 1 (SP, PBL, LR) and Model 1 to Model 5 from SR. For the next 10 cases we start from Model 2 MP and repeat the previous algorithm. The last 10 cases start from Model 3 MP. Two 72 hours forecasts were performed one starting on 06/01/2010 and the other starting on 06/11/2010. These choices covered mean global irradiance in the range 200-410 W/m^2, that is from point cloudiness index ~1 to point cloudiness index ~0. Figures 4 and 5 illustrate the relative random mean square error r-RMSE obtained for the five stations in the forecasting periods already mentioned.

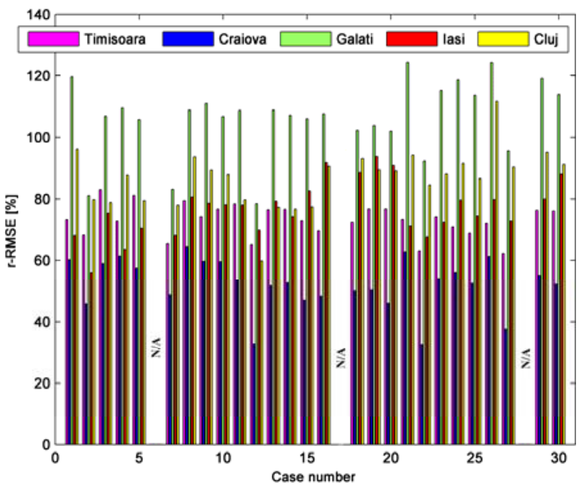

Fig. 4 - Distribution of the r-RMSE in 5 stations. Mean experimental GHI [W/m^2]: Timisoara: 208; Craiova: 302; Galati: 249; Iasi: 299; Cluj: 233. N/A means that code failed to produce results beyond 30 hours of forecast for respective cases.

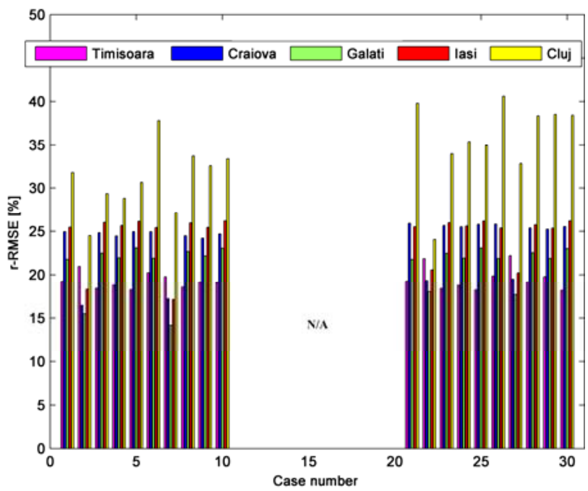

Fig. 5 - Distribution of the r-RMSE in 5 stations. Mean experimental GHI [W/m^2]: Timisoara: 405; Craiova: 404; Galati: 433; Iasi: 398; Cluj: 382. N/A means that code failed to produce any results for respective case range.

The results show the existance of potential cases to be considered in assessing the best combination of switches that produce the smallest r-RMSE value for the ensamble of 47x5=230 cases. At the same time and quite unexpectedly, there is a number of combinations that fail either to produce any results or to complete the full 72 hours forecast. More intriguing is that, although cases 11-20 (except case 17) worked well for the first forecast period (06/01/2010-06/03/2010), when the point cloudiness substantially decreases during the second forecast period (06/11/2010-06/13/2010) the same cases fail to make even a time step. In this situation code hangs on and must be aborted. The most important cases that emerged from our analysis are presented in Table 3.

Table 3

Number of the first four most favorable cases for both forecasting sessions

	06/01 First rank	06/11 First rank	06/01 Second rank	06/11 Second rank	06/01 Third rank	06/11 Third rank	06/01 Fourth rank	06/11 Fourth rank
Timisoara	27	30	22	25	12	5	7	23
Craiova	22	2	12	7	27	22	2	27
Galati	12	7	2	2	7	27	22	22
Iasi	2	7	4	2	22	27	1	22
Cluj	12	22	14	2	13	7	15	4

One can immediately see that there are 5 more frequent cases present in the table above: 2, 7, 12, 22 and 27.

Based on the above data, we can build up an objective function associated with case Ψ_i whose maximum is sought for. We consider the following weights w_i for each place: 1 for first place, 0.8 for the second, 0.6 for third and 0.4 for the last place each case has achieved.

$$\Psi_i = \sum_{1}^{4} w_i, i = 1 \dots 5 \tag{2}$$

The value of each objective function is contained in Table 4.

Table 4

Values of the objective function

	Case 2	Case 7	Case 12	Case 22	Case 27
Ψ	5.6	5	3.4	5.2	3.2

We found out that combination 2 had the best performance for both forecasting sessions. Anyway, what is important to recognize is that all best cases are related to GFDL shortwave radiation model.

6. Conclusions

Our preliminary model analysis of WRF performance shows that the accuracy of the computed global solar irradiance can be improved by choosing the appropriate physics models. Table 4 shows that combination 2 provides the best results. In order to draw a definite conclusion more work has to be done to extend our analysis by considering a larger collection of physics models.

Acknowledgements

The authors thank Dr. Cristian Oprea and Dr. Alexandru Dumitrescu (National Meteorological Administration) for previous collaboration when measurements database was prepared. This work was supported by a grant of the Romanian National Authority for Scientific Research, CNCS - UEFISCDI, project number PN-II-ID-PCE-2011-3-0089 and by the European Cooperation in Science and Technology project COST ES1002.

References

[1] Heinemann D., Lorenz E., Girodo M. (2006). *Forecasting of solar radiation* in: Dunlop, E.D., Wald, L., Suri, M. (Eds.), *Solar Energy Resource Management for Electricity Generation from Local Level to Global Scale*. Nova Science Publishers, Hauppauge.

[2] Mellit A., Pavan A.M. (2010). Sol. Energy 84 (5), (pp. 807–821)

[3] IEA, (2007). *Energy Technologies at the Cutting Edge*, International Energy Agency, OECD Publication Service, OECD, Paris.

[4] Grell G., Dudhia J., Stauffer D. (1998). A Description of the Fifth-Generation Penn State/NCAR Mesoscale Model (MM5), NCAR Tech. Note, NCAR/TN-398+STR, USA,.

[5] Zamora R.J., Dutton E.G., Trainer M., McKeen S.A., Wilczak J.M., Hou Y.T. (2005). *Mon. Weather Rev*. 133, (pp. 783–792).

[6] Zamora R.J., Solomon S., Dutton E.G., Bao J.W., Trainer M., Portmann R.W., White A.B., Nelson D.W., McNider R.T. (2003). J. Geophys.Res. 108 (D2), 4050.

[7] Lorenz E., RemundJ., Muller S.C., Traunmuller W., Steinmaurer G., Pozo D., Ruiz-Arias J.A., Fanego V.L., Ramirez L., Romeo M.G., Kurz C., Pomares L.M., Guerrero C.G. (2009). Benchmarking of different approaches to forecast solar irradiance. In: 24th European Photovoltaic Solar Energy Conference, Hamburg, Germany.

[8] Lorenz E., Hurka J., Heinemann D., Beyer H.G. (2009). IEEE J. Selected Topics Appl. Earth Observations Remote Sens. 2 (1).

[9] Remund R., Perez Y., Lorenz E. (2008). Comparison of solar radiation forecasts for the USA. In: Proceedings of the 23rd European Photovoltaic Solar Energy Conference, Valencia, Spain, (pp. 1.9–4.9).

[10] Perez Y., Ramos-Real F.J. (2009). Renew. Sust. Energy Rev., 13, (pp. 1058–1066).

[11] Ruiz-Arias J.A., Pozo-Vazquez D., Sanchez-Sanchez N., Montavez J.P., Hayas-Barru A., Tovar-Pescador J., Il Nuovo Cimento, 31 (5–6), (pp. 825–842).

[12] D. Santos-Muñoz, J. Wolff, C. Santos, García-Moya J.A., Nance L. (2009). Implementation and validation of WRF model as ensemble member of a probabilistic prediction system over Europe. In: 10th Annual WRF Users' Workshop, Boulder, CO.

[13] ARW version3 Modeling System User's Guide. (2012). National Center for Atmospheric Research, http://www.mmm.ucar.edu/wrf/users/docs/user_guide_V3/contents.html.

[14] Skamarock W.C., Klemp J.B., Dudhia J., Gill D.O., Barker D.M., Duda M.G., Huang X.Y., Wang W., Powers, J.G. (2008). A description of the advanced research WRF Version 3. NCAR/TN-475+STR.

[15] Dudhia J. (1989). Numerical study of convection observed during the winter monsoon experiment using a mesoscale two-dimensional model, J. Atmos. Sci., 46, (pp. 3077–3107).

[16] Chou M.D., Suarez M.J. (1994). *An efficient thermal infrared radiation parameterization for use in general circulation models.* NASA Tech. Memo. 104606, 3, pp. 85.

[17] Collins, W.D. et al. (2004) Description of the NCAR Community Atmosphere Model (CAM 3.0), NCAR Technical Note, NCAR/TN-464+STR, pp. 226.

[18] Mlawer, E. J., Taubman S. J., Brown P. D., Iacono M. J., Clough S. A. (1997) Radiative transfer for inhomogeneous atmosphere: RRTM, a validated correlated-k model for the longwave. J. Geophys. Res., 102 (D14), (pp. 16663–16682).

[19] Chou M.D., Suarez M. J. (1999) A solar radiation parametrization for atmospheric studies, NASA/TM-1999-104606, Vol. 15.

[20] Lacis A. A. and Hansen J. E. (1974). A parameterization for the absorption of solar radiation in the earth's atmosphere, J. Atmos. Sci., 31, (pp. 118–133).

[21] Dudhia J. *Overview of WRF Physics*, http://www.mmm.ucar.edu/wrf/users/tutorial/201201/Physics _Dudhia .ppt.pdf

[22] Stephens G. L. (1978). *Radiation profiles in extended water clouds. Part II: Parameterization schemes, J. Atmos. Sci.*, 35, (pp. 2123–2132).

[23] Badescu V., Dumitrescu A. (2013). The CMSAF Hourly Solar Irradiance Database (Product CM54). Accuracy And Bias Corrections With Illustrations For Romania (South-Eastern Europe), Journal of Atmospheric and Solar-Terrestrial Physics, 93, (pp. 100-109).